Sit-to-stand-and-walk from 120% Knee Height: A Novel Approach to Assess Dynamic Postural Control Independent of Lead-limb

Gareth D. Jones[1,2], Darren C. James[3], Michael Thacker[1,2], David A. Green[1]

[1]Centre for Human and Aerospace Physiological Sciences (CHAPS), Faculty of Life Sciences and Medicine, King's College London

[2]Physiotherapy Department, Guy's & St Thomas' NHS Foundation Trust, London

[3]School of Applied Sciences, London South Bank University

Correspondence to: Gareth D. Jones at gareth.jones@gstt.nhs.uk

Abstract

Individuals with sensorimotor pathology *e.g.,* stroke have difficulty executing the common task of rising from sitting and initiating gait (sit-to-walk: STW). Thus, in clinical rehabilitation separation of sit-to-stand and gait initiation - termed sit-to-stand-and-walk (STSW) - is usual. However, a standardized STSW protocol with a clearly defined analytical approach suitable for pathological assessment has yet to be defined.

Hence, a goal-orientated protocol is defined that is suitable for healthy and compromised individuals by requiring the rising phase to be initiated from 120% knee height with a wide base of support independent of lead limb. Optical capture of three-dimensional (3D) segmental movement trajectories, and force platforms to yield two-dimensional (2D) center-of-pressure (COP) trajectories permit tracking of the horizontal distance between COP and whole-body-center-of-mass (BCOM), the decrease of which increases positional stability but is proposed to represent poor dynamic postural control.

BCOM-COP distance is expressed with and without normalization to subjects' leg length. Whilst COP-BCOM distances vary through STSW, normalized data at the key movement events of seat-off and initial toe-off (TO1) during steps 1 and 2 have low intra and inter subject variability in 5 repeated trials performed by 10 young healthy individuals. Thus, comparing COP-BCOM distance at key events during performance of an STSW paradigm between patients with upper motor neuron injury, or other compromised patient groups, and normative data in young healthy individuals is a novel methodology for evaluation of dynamic postural stability.

Video Link

The video component of this article can be found at https://www.jove.com/video/54323/

Introduction

Clinical pathologies affecting the sensorimotor systems, for example upper motor neuron (UMN) injury following stroke, lead to functional impairments including weakness, loss of postural stability and spasticity, which can negatively affect locomotion. Recovery can be variable with a significant number of stroke survivors failing to achieve the functional milestones of safe standing or walking[1,2].

The discrete practice of walking and sit-to-stand are common rehabilitative tasks after UMN pathology[3,4], however transitional movements are frequently neglected. Sit-to-walk (STW) is a sequential postural-locomotor task incorporating sit-to-stand (STS), gait initiation (GI), and walking[5].

Separation of STS and GI, reflective of hesitation during STW has been observed in patients with Parkinson's disease[6] and chronic stroke[7], in addition to older unimpaired adults[8], but not in young healthy individuals[9]. Therefore sit-to-stand-and-walk (STSW) is commonly implemented within the clinical environment and is defined by a pause phase of variable length when standing. However, there are no published protocols to date defining STSW dynamics in a context suitable for patient populations.

Usually in STW studies the initial chair height is 100% of knee height (KH; floor-to-knee distance), foot-width and GI lead-limb are self-selected, arms are constrained across the chest and an ecologically meaningful task context is often absent[5-9]. However, patients find rising from 100% KH challenging[10] and frequently adopt a wider foot position compared with healthy individuals[11], initiate gait with their affected leg[7], and use their arms to generate momentum[7].

To initiate gait, a state change in whole-body movement in a purposeful direction is required[12]. This is achieved by uncoupling the whole-body center-of-mass (BCOM: the weighted average of all considered body segments in space[13]) from the center-of-pressure (COP: the position of the resultant ground reaction force (GRF) vector[14]). In the anticipatory phase of GI, rapid stereotypical posterior and lateral movement of the COP

toward the limb to be swung occurs thereby generating BCOM momentum[12,15]. The COP and BCOM are thus separated, with the horizontal distance between them having been proposed as a measure of dynamic postural control[16].

The calculation of COP-BCOM distance requires simultaneous measurement of the COP and BCOM positions. The standard calculation of COP is shown below in equation (1)[17]:

$$COP_x = \frac{((Origin_z * Force_x) - M_y)}{Force_z}$$

$$COP_y = \frac{(M_x + (Origin_z * Force_y))}{Force_z}$$

$$COP_z = Origin_z$$
(1)

Where M and Force represent moments about the force platform axes and the directional GRF respectively. The subscripts represent axes. The origin is the vertical distance between the contact surface and the origin of the force platform, and is considered to be zero.

The kinematic method of deriving BCOM position involves tracking the displacement of segmental markers. A faithful representation of body-segment motion can be achieved by employing markers clustered on rigid plates placed away from bony landmarks, minimizing soft-tissue-artifact (CAST technique[18]). In order to determine BCOM position, individual body segment masses are estimated, based on cadaveric work[19]. Three-dimensional (3D) motion system proprietary software uses the coordinate positions of proximal and distal segment locations to: 1) determine segmental lengths, 2) arithmetically estimate segmental masses, and 3) compute segmental COM locations. These models are then able to provide estimates of 3D BCOM position at a given point in time based on the net summation of inter-segmental positions (**Figure 1**).

Thus, the purpose of this paper is first to present a standardized STSW protocol that is ecologically valid and includes rising from a high seat-height. It has been shown previously that STSW from 120% KH is biomechanically indistinct from 100% KH barring generation of lower BCOM vertical velocities and GRF's during rising[20], meaning rising from 120% KH is easier (and safer) for compromised individuals. Second, to derive COP-BCOM horizontal distances to assess dynamic postural control during key milestones and transitions using 3D motion-capture. This approach, which in healthy individuals during STSW is independent of limb-lead[20], offers the prospect of functional recovery evaluation. Finally, a preliminary STSW data set representative of young healthy individuals is presented, and intra and inter-subject variability in the group is defined in order to inform comparison with pathological individuals.
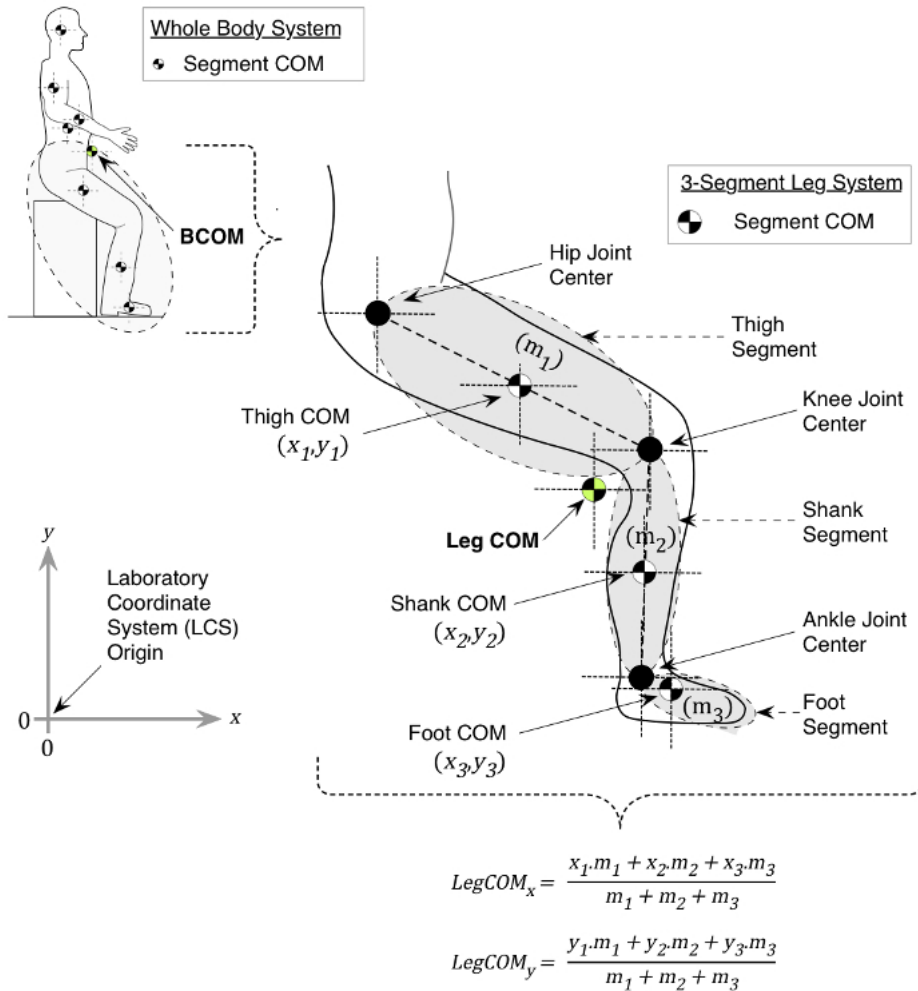
Figure 1. 2D BCOM calculation. For simplicity, the example is based on calculating whole-leg COM from a 3-linked mass in 2 dimensions, where coordinates of the respective COM positions (*x,y*), and segmental masses (m_1, m_2, m_3) are known. Segment masses and location of segmental COM positions, with respect to the laboratory coordinate system (LCS; origin: 0, 0), are estimated by motion analysis system proprietary software using subject body mass and published anthropometric data (see main text). The *x* and *y* leg COM position, in this example of the 3-linked mass, is then derived using the formulae shown. Please click here to view a larger version of this figure.

The display equations shown in the figure:

$$LegCOM_x = \frac{x_1 \cdot m_1 + x_2 \cdot m_2 + x_3 \cdot m_3}{m_1 + m_2 + m_3}$$

$$LegCOM_y = \frac{y_1 \cdot m_1 + y_2 \cdot m_2 + y_3 \cdot m_3}{m_1 + m_2 + m_3}$$

Protocol

The protocol follows the local guidelines for the testing of human participants, defined by London South Bank University research ethics committee approval (UREC1413/2014).

1. Gait Laboratory Preparation

1. Clear the capture volume of unwanted reflective objects that may be misinterpreted as movement markers and eliminate ambient daylight to reduce reflections as appropriate.
2. Turn on motion-capture cameras, proprietary tracking software, force platform amplifiers, and external analogue-to-digital (AD) converter. Allow time for the cameras to initialize.
3. Arrange cameras ensuring that there are at least 2 intersecting axes at the extremes of the capture volume. Ensure individual cameras have optimal exposure and aperture settings by checking individual point-resolution of test markers (*e.g.,* the static calibration frame) within capture volume space (see Reference Appendix A[21]).
4. Mount subject-switch to turn off visual go signal in the midline of the walkway, 6 m in front of the starting position in the direction of travel, on a tripod at subject's navel height. Mount light source (for visual go signal) in the midline of the walkway, 1 m in front of the subject-switch in the direction of travel, on a tripod at subject's canthus height (**Figure 2**). Arrange the operator light switch in close proximity to the investigator.
5. Arrange force platforms 1 and 2 in parallel for gait-initiation, and force platforms 3 and 4 in a staggered configuration to capture non-dominant lead-limb trials. Then attach force platform covers with removable tape.
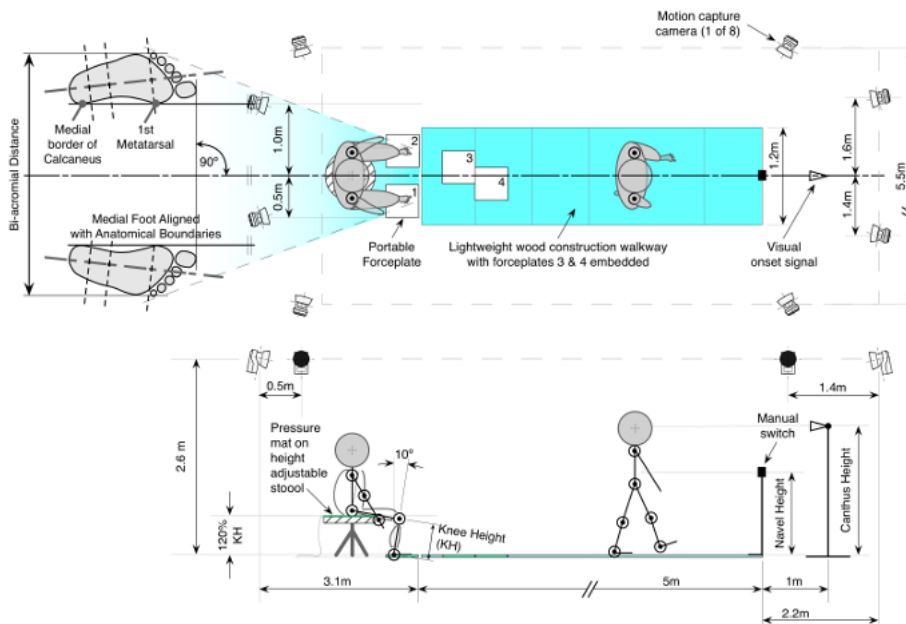
Figure 2. Experimental Protocol. This example shows a left-leg lead: Subjects sit on an instrumented stool at 120% knee height (KH) with ankles 10° degrees in dorsiflexion and feet at shoulder width apart orientated forward. On a visual cue, subjects perform 5 trials of STSW leading with their non-dominant limb at self-selected pace terminated by switching off the light. Please click here to view a larger version of this figure.

6. In the proprietary tracking software set capture frequency to 60 Hz and 3D tracking parameters. Specifically, use a prediction error of 20 mm, a maximum residual of 2 mm, minimum trajectory length equivalent to 2 frames, and a maximum frame gap of 10 frames. Go on to identify each of the 8 individual force platform components (z_1, z_2, z_3, z_4, x1-2. x3-4, y1-4, y2-3) from each form platform amplifier into the respective analog to digital converter (32 channels in this study).
    1. Ensure all pre-determined calibration settings from each force platform's calibration documentation, scaling factors and analogue channels have been specified (see chapter Project Options; Analogue Boards[21]) and nominate offset to be read during the last 10 frames of capture when unloaded.

7. In the proprietary tracking software, nominate a multiplier to the motion-capture frequency to ensure an adequate analogue sampling frequency. Use a multiplier of 17, yielding an individual force platform sampling frequency of 1,020 Hz.
8. Implement the dynamic wand calibration procedure:
    1. Position the L-shaped reference structure on the floor in the capture volume in preparation for the calibration of 3D space. The long axis of this structure should be pointing in the anterior direction. (see chapter Wand calibration method[21]).
    2. In the **Calibration settings** page in the **Project options** dialog, select the calibration 'type' to Wand, with a 750 mm length. Then select coordinate system orientation with positive z-axis pointing upwards and positive y-axis as the long arm (see chapter Calibration[21]). Click **OK**.
    3. Click the **Calibration icon** and set the intended length of the calibration capture to 60 sec. Then set a time delay of 5 sec and identify the file directory where the results will be saved. Click **OK** to commence calibrating.
    Note: The wand procedure uses two calibration objects to calibrate the measurement volume; this is used to maximize the resolution of a large motion capture volume (**Figure 3**). One is a stationary L-shaped reference structure with four markers attached to it and is used to define the global coordinate system. The other object is a wand, which consists of two markers located a fixed distance from each other. During calibration, the x, y, z orientations of these are tracked with respect to the x, y, z positions of the four static markers on the reference structure; in turn permitting the proprietary software to triangulate, predict and reconstruct the trajectories of the moving markers in 3D space. At the end of this process, each camera will return a residual error of its accuracy.
    4. Move the calibration wand within the calibration volume by rotating and translating the wand around the intended capture volume for the specified 60 sec (see chapter Wand Calibration Method[21]).
    5. Check the **Calibration results**, accept calibration with individual camera residual errors of < 1.5 mm, click **OK**.
    Note: If you have force plates there will be a warning reminding you of measuring the force plate position again (since it has most probably changed with the new calibration).
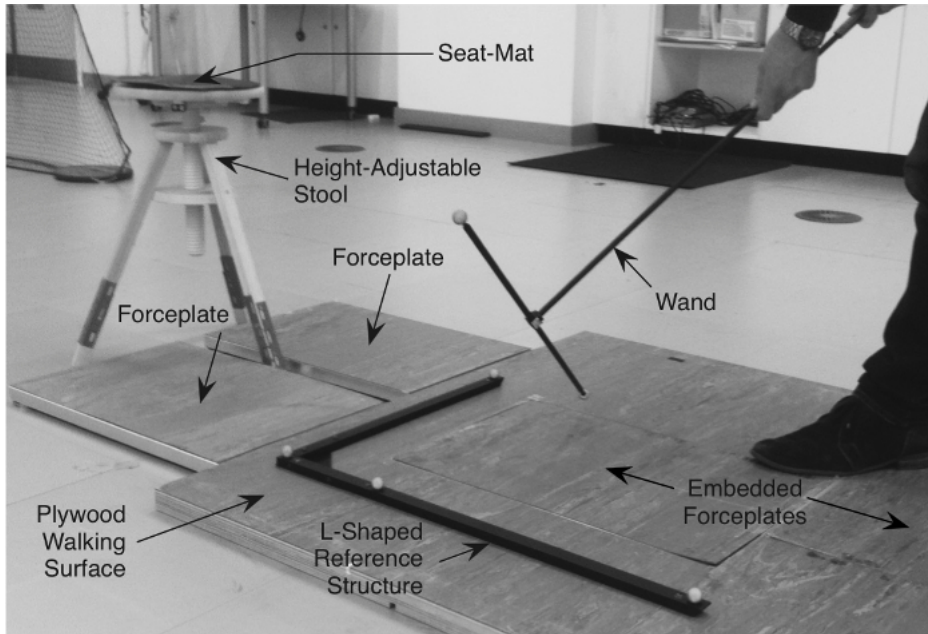
Figure 3. L-Shaped Reference Structure and Wand for Camera Calibration. The L-shaped reference structure remains stationary and has 4 markers attached to it. The wand has two markers attached to it at a fixed distance and is moved, with respect to the reference structure, to create a 3-D calibrated volume of space that is sufficient enough for the intended marker set to pass through. Please click here to view a larger version of this figure.

9. Remove calibration set from capture volume. Locate the force platforms in the calibrated 3D space by placing one 9 mm diameter passive retro-reflective marker in each of the 4 corners of each platform (attention to placement is essential; see chapter Force Plate Location[21]). Obtain a 5 sec recording and proceed to identify each marker and each platform's reference system (PRS) within the 3D space as per proprietary software suggestions.
10. Undertake a dynamic capture using the aforementioned sampling and 3D tracking parameters (1.6) to confirm and sense-check subsequent force magnitudes and directions.
    1. Set up dynamic capture for 15 sec with a 5 sec delay. Once the click to **commence capture** is initiated, the operator has time to sit on the stool, pause, stand, pause and walk forwards making contact with the force platforms (at this point, there is no need for the operator to have retro-reflective markers attached *in situ*).
    2. Once the capture has finished, check the direction and magnitudes of ground reaction vectors to ensure configurations of force-platforms are correct. Expect upward and posterior to direction of travel vectors at foot contact, and a maximum vertical force of approximately 1 to 1.5 times body weight.

11. Place height adjustable stool in the midline of the capture volume between force platforms 1 and 2 (**Figure 2**), then connect a 300 mm diameter pressure seat-mat to the external AD converter.
12. Prepare all passive retro-reflective anatomical markers for fixation by pre attaching individually to one side of double adhesive tape, approximately 15 mm in length (at least 60 cm of double adhesive tape in total per subject) and arrange in an appropriate location ready for application to subject. Include tracking marker clusters and self-securing bandage ready for timely subject application.
    Note: Tracking markers should comprise a minimum of 3 retro-reflective markers arranged in a non-co-linear arrangement, and are placed on body segments (some anatomical markers positioned at estimated joint centers can be used as tracking markers *e.g.,* 1st and 5th metatarsals).

2. Subject Preparation

1. Obtain written informed consent from subject who fulfills inclusion/exclusion criteria.
2. Ask subject to change into suitable clothing (cycling shorts, close fitting t-shirt and sports bra as appropriate).
3. Establish dominant lower limb using the kicking-a-ball test[22] if the subject is able to safely do so.
4. Measure subject standing height (m) and mass (kg); convert mass to weight (N).
5. With subject standing, measure subject bi-acromial distance (m) using measuring calipers. Lock caliper position to use distance for feet positioning (see 4.5 below).
6. Measure vertical floor-to-knee distance (m) on the dominant limb (in standing); multiply distance by 1.2 to calculate 120% KH distance (m). Adjust stool height to 120% KH. **Table 1** summarizes 10 healthy subject characteristics including knee height data.

Subject	Gender	Dominant Leg	Age (years)	Knee Height (m)*	120% KH (m)	Mass (kg)	Height (m)	Dom Leg Length (m)†
1	F	R	21	0.430	0.516	51.9	1.653	0.806
2	F	L	25	0.450	0.540	73.7	1.662	0.836
3	F	R	30	0.451	0.541	65.1	1.657	0.823
4	M	R	46	0.420	0.504	69.2	1.670	0.803
5	F	R	35	0.498	0.598	77.5	1.711	0.892
6	M	R	26	0.540	0.648	89.7	1.900	0.976
7	M	R	34	0.460	0.552	77.3	1.690	0.856
8	M	R	27	0.474	0.569	86.5	1.762	0.870
9	F	R	27	0.424	0.509	67.5	1.633	0.834
10	M	R	20	0.465	0.558	76.5	1.759	0.851
–	–	–	29.1 (±7.7)	0.461 (±0.036)	0.553 (±0.044)	73.5 (±10.9)	1.701 (±0.080)	0.885 (±0.051)

* Distance from medial knee joint line to floor on dominant side
†Distance from hip joint center to floor on dominant side

Table 1: Subject Characteristics. Individual data and mean (±1 SD) across 10 subjects are shown.

7. Prepare the skin areas for marker placement. Shave unwanted body hair as appropriate and use alcohol wipes to remove excess sweat and/ or moisturizer to maximize adherence between markers and the skin.
8. Palpate, identify and apply retro-reflective markers to anatomical landmarks of the lower and upper extremities, trunk, head and pelvic segments using double adhesive tape in accordance with the chosen technical frame of reference[23] (**Table 2**). Go on to apply segmental tracking markers with self-securing bandage.
   Note: In females, if difficulty arises locating the sternal notch marker - place marker over the center of the sports bra garment.

Segment	Label	No	Static	Dynamic	Descriptor
Head	TMJ	2	✓	✗	Temporomandibular joint
	VERT1	1	✓	✓	Vertex
	VERT2	1	✓	✓	Head tracking marker 2
	VERT3	1	✓	✓	Head tracking marker 3
Torso	JN	1	✓	✓	Most caudal aspect of jugular notch
	XP	1	✓	✓	Xiphoid process
	C7	1	✓	✓	Dorsal aspect of 7th cervical vertebra spinous process
	T8	1	✓	✓	Dorsal aspect of 8th thoracic vertebra spinous process
Pelvis	ASIS	2	✓	✓	Anterior superior iliac spine
	PSIS	2	✓	✓	Posterior superior iliac spine
Humerus	MHU	2	✓	✗	Medial humeral epicondyle
	LHU	2	✓	✗	Lateral humeral epicondyle
	AC	2	✓	✓	Acromioclavicular Joint
	HUM1	2	✓	✓	Humerus tracking marker 1
	HUM2	2	✓	✓	Humerus tracking marker 2
	HUM3	2	✓	✓	Humerus tracking marker 3
Forearm	RSY	2	✓	✗	Radial styloid process
	USY	2	✓	✗	Ulnar styloid process
	FRM1	2	✓	✓	Forearm tracking marker 1
	FRM2	2	✓	✓	Forearm tracking marker 2
	FRM3	2	✓	✓	Forearm tracking marker 3
Thigh	LEP	2	✓	✗	Lateral femoral epicondyle
	MEP	2	✓	✗	Medial femoral epicondyle
	THIGH1	2	✓	✓	Thigh tracking marker 1
	THIGH2	2	✓	✓	Thigh tracking marker 2
	THIGH3	2	✓	✓	Thigh tracking marker 3
	THIGH4	2	✓	✓	Thigh tracking marker 4
Shank	LML	2	✓	✗	Lateral malleolus
	MML	2	✓	✗	Medial malleolus
	TTB	2	✓	✗	Tibial tuberosity
	HFB	2	✓	✗	Fibula head
	SHANK1	2	✓	✓	Shank tracking marker 1
	SHANK2	2	✓	✓	Shank tracking marker 2
	SHANK3	2	✓	✓	Shank tracking marker 3
	SHANK4	2	✓	✓	Shank tracking marker 4
Foot	CAL	2	✓	✓	Upper ridge of the calcaneus posterior surface
	FM	2	✓	✓	First metatarsal
	VM	2	✓	✓	5th metatarsal
	SM	2	✓	✗	2nd metatarsal
	Individual Markers:	40	16		
	Cluster Markers:	31	31		
	Total:	71	47		

Table 2: Marker-set placement. Markers (anatomical and tracking) based on a previously reported technical frame of reference[23].

9. Ask subject to walk into the capture volume and adopt the anatomical position. At this point the subject must not move until after static capture has been performed due to the inherent problem of estimating the hip joint center over clothing at this anatomical location.

3. Static Capture

1. Instruct subject to stand stationary in the center of the capture volume, assuming the standard anatomical position, with all anatomical and tracking markers *in situ*.
   Note: In order to reduce soft tissue artifact a static calibration is undertaken with anatomical and tracking markers *in situ*. The tracking markers are referenced to the anatomical markers, which negates the limitation of assuming that joint centers do not move under the skin. Tracking markers are left *in situ* for subsequent dynamic trials. This is termed the calibrated anatomical systems technique (CAST)[18].
   1. In order to undertake a short static capture, use the aforementioned sampling and 3D tracking parameters (1.6) and ensure all markers are accounted for in the capture volume by confirming the total number of markers listed in the **Unidentified Trajectories** panel in 3D

real-time mode. This should correspond with the total number of markers that the chosen technical frame of reference requires. Click the **record icon** to complete a 5 sec capture. Repeat procedure where necessary if markers are missing.
Note: See section 6 below for the processing of static capture data.

2. Use the position data from the hip-joint-center landmark on the subject dominant side to determine leg-length (distance from hip-joint-center (see 7.1 and Table 3b below) to floor) for distance normalization (see 7.11 below).

4. Familiarization

1. Remove all anatomical-only markers.
2. Instruct subject to sit on the stool with feet on individual force platforms 1 & 2.
3. Instruct subject to stand and then walk forward with the defined leading leg. Adjust the anteroposterior position of the stool until the subject consistently makes central contact with force platforms 3 and 4 during the first 2 steps of gait. Allow repeated practice trials until the subject is comfortable.
4. Mark the front leg position of the stool with tape on the floor surface in order to re-establish stool position.
5. Set up final feet position (**Figure 2**). Ask subject to sit on the stool with feet on individual force platforms 1 and 2. Adjust shank position on subject's dominant side 10° posterior from vertical using an extendable arm goniometer. Go on to adjust the non-dominant foot equally in line, and then using the locked calipers (see 2.5 above), arrange the inter-foot width to the pre-determined bi-acromial distance accordingly between the lateral foot borders.
6. Adjust the transverse plane orientation of each foot such that each medial foot border is placed in line with the direction of travel.
7. After finally checking alignment, draw around final foot positions using a dry board marker pen onto the removable force platform surface.
8. Use the verbal instruction: "When you see the light come on in front of you, stand up and stop. Mentally count down from 3 to 1, one number at a time. Then, leading with your non-dominant leg, walk at a comfortable pace toward the switch in front of the light and stop. Count mentally from 3 down to 1, one number at a time, and then with your writing hand use the switch to turn off the light".
9. Re-iterate to the subject that they may use their arms naturally, then allow the subject sufficient familiarization to STSW protocol. Familiarization gives the subject as much time as possible to acclimatize to the testing environment ensuring they are able to efficiently accomplish the task without any forced movement that might otherwise impinge on the ecological validity of the experimental paradigm.

5. STSW Dynamic Trials

1. With subject sitting on the stool ready for dynamic trials, first confirm the total number of markers listed in the **Unidentified Trajectories** panel in 3D real-time mode and that they correspond with the total number of markers that the chosen technical frame of reference requires. Then click the **record icon** to complete a 15 sec dynamic capture.
2. After 5 sec capture, turn on the operator light-switch and check how the subject responds - that they rise from the stool and pause as instructed, step on to force platforms 3 and 4, and that they stop and turn the light off as instructed within the capture period.
3. Re-set the light switch and check for marker dropouts by accounting for all markers during slow motion playback of trial. Repeat if necessary, otherwise continue to next trial. Go on to capture 5 trials of STSW in each subject.
4. In the event of anatomical markers becoming unattached, re-attach to predetermined skin mark. If tracking markers move, re-attach anatomical markers and repeat static trial - then continue with remaining dynamic trials.

6. Proprietary Tracking Software Post Processing

1. In proprietary tracking software, identify and label all markers from static and dynamic trials (see chapter Manual Identification of Trajectories[21]) and crop unwanted capture by moving the time-slides to the beginning and end of the task. Utilize the "automatic identification of markers", otherwise known as **AIM**, functionality in the proprietary tracking software to aid labeling (see chapter Generating an AIM Model[21]).
Note: Labeling of markers is required so that the proprietary and subsequent biomechanics analysis software consistently constructs and calculates the relative trajectory of a rigid body in 3-dimensional space. Use meaningful labeling as shown in **Table 2**. **AIM** is subject-specific, but continually updates. With a different subject and in the event of a poor AIM, go on to update **AIM** by manual labelling. This also applies to the static capture process (see section 3.1.1 above).
2. In the event of marker drop out, that exceeds 10 frames, go on to either locate the missing trajectory in the **Unidentified Trajectories** panel, or manually **gap-fill** using the polynomial interpolation function provided by the proprietary software (see chapter Gap Fill Trajectories[21]).
Note: In some cases marker trajectories are partially absent and gap-filling is a mechanism whereby missing data can be mathematically estimated based on the measured trajectory before and after the missing data.
3. Format and export all static and dynamic trials, in **c3d** format, for post-processing in biomechanics analysis software.
Note: Prior to export, exclude all unidentified and empty marker trajectories, specifying de facto labeling, and nominate the last 10 frames for zero force baseline levels for each force plate.

7. Biomechanics Analysis Software Post Processing

1. Build static 13-segment model[23] (feet, shanks, thighs, pelvis, trunk, upper arms, forearms and head (note no hands)).
Note: The process of model building is fundamental in defining the linked segments based on the static measurement trial and proprietary software instructions were used[24]. In this protocol the anatomical coordinate systems for each body segment (**Table 3a**) and joint center locations (**Table 3b**) are based mainly on Ren *et al.*[23] with adaptations to avoid functional hip and glenohumeral joint center estimation. Gold standards for all joint center locations remain imaging techniques such as magnetic resonance imaging (MRI), which are unrealistic in most situations. Functional joint center estimations have been utilized; however, there remains the risk that patients with pathology would not be

able to move the joint in the requisite planes[25]. Therefore, for the pelvis regression equations *e.g.,* Davis[26] are often used. Here, the CODA pelvis[27] was used and is based on work by Bell *et al.*[28], and the glenohumeral joint centers were estimated according to Eames *et al.*[29].

Segment	Origin	Axes		
		x	*y*	*z*
Foot	Upper ridge of calcaneus (CAL)	Coincides with intersection between plane defined by CAL, 1st and 5th metatarsals (FM and VM), and its perpendicular plane containing CAL and 2nd metatarsal (SM), pointing forward	Mutually perpendicular to both *x*- and *z*-axis pointing upwards	Perpendicular to *x*-axis in plane defined by CAL, FM and VM pointing right
Shank	Midpoint between lateral and medial malleolus (LMAL and MAML)	Mutually perpendicular to both *y*- and *z*-axis pointing forward	Coincides with intersection between plane defined by fibula head (HFB), LMAL and MMAL, and its perpendicular plane containing tibial tuberosity (TTB) and midpoint between LMAL and MMAL,	Perpendicular to *y*-axis in plane defined by HFB, LMAL and MMAL pointing right
Thigh	Midpoint between lateral and medial epicondyles (LEP and MEP)	Mutually perpendicular to both *y*- and *z*-axis pointing forward	Oriented from midpoint between LEP and MEP to hip joint center (HJC) pointing upwards	Perpendicular to y-axis in plane defined by LEP, MEP and HJC pointing right
Pelvis	Midpoint between right and left anterior superior iliac spine (RASIS and LASIS)	Perpendicular to z-axis in plane defined by RASIS, LASIS and midpoint between right and left posterior superior iliac spine (RPSIS and LPSIS)	Mutually perpendicular to both *x*- and *z*-axis pointing upwards	Oriented from LASIS to RASIS pointing right
Torso	Jugular notch (JN)	Perpendicular to *y*-axis in plane defined by C7, JN and midpoint between T8 and XP	Oriented from midpoint between JN and C7, and midpoint between T8 and xiphoid process (XP), pointing upwards	Mutually perpendicular to both *x*- and *y*-axis pointing right
Humerus	Shoulder joint center (SJC)	Mutually perpendicular to both *y*- and *z*-axis pointing forward	Oriented from midpoint between medial and lateral humeral epicondyles (MHU and LHU) to SJC pointing upwards	Perpendicular to *y*-axis in plane defined by MHU, LHU and SJC pointing right
Forearm	Midpoint between radial styloid (RSTY) and ulnar styloid (USTY)	Mutually perpendicular to both *y*- and *z*-axis pointing forward	Oriented from midpoint between RSTY and USTY to elbow joint center (EJC) pointing upwards	Perpendicular to *y*-axis in plane defined by RSTY, USTY and EJC pointing right
Head	Midpoint between right and left temporomandibular joints (RTMJ and LTMJ)	Mutually perpendicular to both *y*- and *z*-axis pointing forward	Oriented from origin to vertex (VERT1) pointing upwards	Perpendicular to *y*-axis in plane defined by RTMJ, LTMJ and VERT1 pointing right

Table 3a: Anatomical Coordinate System for Whole Body Model.

Joint	Joint Center Definition
Glenohumeral	30 mm inferior to AC markers
Elbow	Mid point between MHU and LHU markers
Right Hip	x : 0.36*Distance between left and right ASIS
	y : 0.19*Distance between left and right ASIS
	z : 0.3*Distance between left and right ASIS
Left Hip	x : 0.36*Distance between left and right ASIS
	y : 0.19*Distance between left and right ASIS
	z : 0.3*Distance between left and right ASIS
Knee	Mid point between MEP and LEP markers
Ankle	Mid point between MMAL and LMAL markers

Table 3b: Joint Center Definitions for Whole Body Model.

2. Import the dynamic files and assign the model to each. Confirm accuracy of model building by checking normal visual configuration of segments. In the case of inaccuracy, the operator is advised to go back to the proprietary tracking software files and check sensor image tracking profiles and correct as necessary.
3. Low pass filter kinematic and kinetic data using a 4th order Butterworth filter with cut-off frequency at 6 Hz and 25 Hz respectively.
4. Average filter light and pressure-mat analogue signals over a 25-frame window.
5. Create force structure for force platforms 1, 2, 3, and 4. Use corner coordinates to create a level-surfaced, rectangular structure encompassing all 4 force platforms (**Figure 4**).
   Note: A force structure is required[30] in order that net COP calculations can be made across the 4 force platforms.
6. Calculate the net COP coordinate signals (x and y) within the laboratory coordinate system (LCS) from the force structure.
   Note: The software performs this by using equations 2a-g below.
   1. Use x and y signals from equations 2f and 2g for net COP position within the LCS.

(2a) Net medio-lateral force $\quad F_x = \sum^{4} F_{xi}$

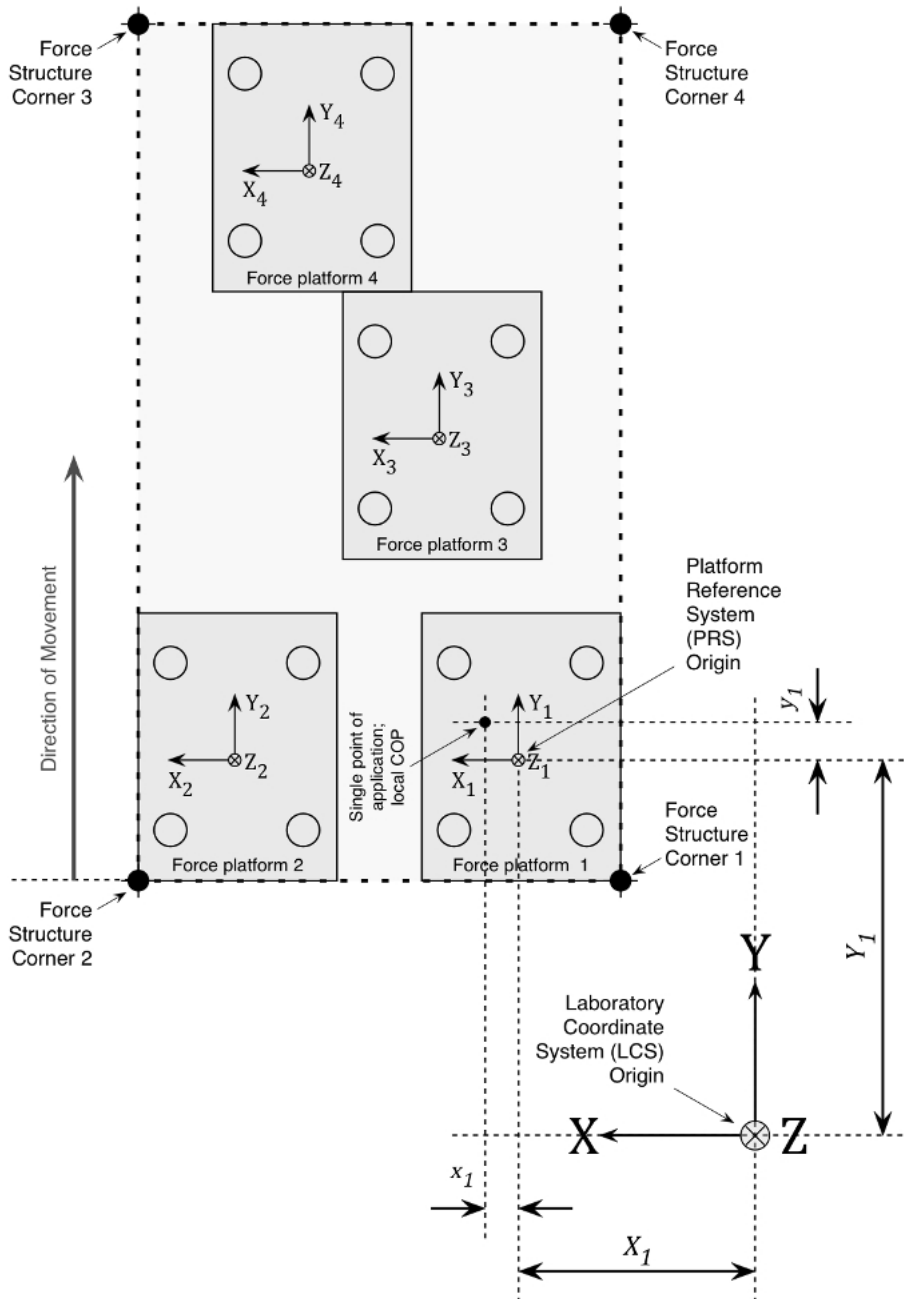(2b) Net anterior-posterior force $\quad F_y = \sum_{i=1}^{4} F_{yi}$

(2c) Net vertical force $\quad F_z = \sum_{i=1}^{4} F_{zi}$

(2d) Net platform moment about x-axis $\quad M_x = \sum^{4} (Y_i + y_i) * F_{zi}$

(2e) Net platform moment about y-axis $\quad M_y = \sum^{4} -(X_i + x_i) * F_{zi}$

(2f) x-Coordinate of net force application point (COP_x) $\quad COP_x = \dfrac{-M_y}{F_z}$

(2g) y-Coordinate of net force application point (COP_y) $\quad COP_y = \dfrac{M_x}{F_z}$

Figure 4. Force Structure. Example of a rectangular force structure encompassing 4 force platforms in a right lead-limb orientation. Details of local COP application and dimensions with respect to a laboratory coordinate system (LCS) are shown for force platform 1 as an example. The *x*, *y*, *z* position of the platform reference system (PRS) is offset relative to the LCS where X_1 and Y_1 represent the mediolateral and anteroposterior distances from PRS, respectively. To calculate the individual platform moment about the *x*-axis, the vertical GRF is multiplied by the sum of the local *y* COP coordinate and the new PRS-LCS offset *y* coordinate (Y_1+y_1). The moment about the *y*-axis coordinate is similarly calculated by multiplying the vertical GRF by the negative sum of the local *x* COP coordinate and the new PRS-LCS offset *x* coordinate -(X_1+x_1). The total moment of force about the global force structure is equal to the sum of all of the moments of force, divided by the sum of the individual vertical forces. Net COP *X* and *Y* coordinates are thus produced for the force structure within the LCS (equations 2a-g). Please click here to view a larger version of this figure.

7. Using customized pipeline commands, create important movement events within STSW, specifically seat-off, upright, gait initiation onset, first toe-off 1, and 1st and 2nd initial contacts (**Table 4**).

Event	Definition
Seat-Off	Instance determined as the point at which the seat-mat analogue channel voltage dropped below the mean-3SDs voltage for >8 frames (133msec) of 1 sec quiet sitting
Upright	Instance of initial peak vertical (z-component) BCOM displacement signal occurring between seat-off and first toe-off events
GI Onset	Instance when COP lateral velocity signal breaches 0.0m/s threshold for > 8 frames (133msec) occurring between Upright and HO1 events
1st Toe-Off	Instance of swing limb force plate vertical (z-component) GRF signal <20N for >8 frames (133msec) occurring after Seat Off event
1st Initial Contact	Instance of force plate 3 vertical (z-component) GRF signal >20N for >8 frames (133msec) occurring after TO1 event
2nd Initial Contact	Instance of force plate 4 vertical (z-component) GRF signal >20N for >8 frames (133msec) occurring after IC1 event

Table 4: Movement Event Definitions. GI – gait initiation; COP – center-of-pressure; HO1 – first heel-off; TO1 – 1st toe-off, IC1 – 1st initial contact.

8. Using customized pipeline commands calculate the COP-BCOM distance (*L*) by applying equation 3 at each movement event, where t_i represents a given event.

$$L(t_i) = \sqrt{[(x_{COP}(t_i)) - (x_{BCOM}(t_i))^2 + (y_{COP}(t_i)) - (y_{BCOM}(t_i))^2]}$$
(3)

9. Using customized pipeline commands, calculate the maximum COP-BCOM distance (*L$_{max}$*) by applying equation 4 between two events ($t_o \rightarrow t_i$).

$$L_{max} = \max_{0 \leq t \leq i}\left\{\sqrt{[(x_{COP}(t_i)) - (x_{BCOM}(t_i))^2 + (y_{COP}(t_i)) - (y_{BCOM}(t_i))^2]}\right\}$$
(4)

where: t_0 and t_i represent movement onset and the final time instance of interest respectively, ($x_{COP}(t_i)$) is the *x* coordinate of the COP at time t_i, ($x_{BCOM}(t_i)$) is the coordinate of the BCOM at time t_i, and ($y_{COP}(t_i)$) and ($y_{BCOM}(t_i)$) are the corresponding values for the *y* coordinates[31].

10. Extract dependent variables of interest at movement events; COP-BCOM distances at seat-off and first toe-off (TO1) events, and maximum COP-BCOM distances during the 1st step phase (between TO1 and first initial-contact; IC1) and the 2nd step phase (between IC1 and IC2) using customized pipeline commands.
11. Normalize intra-subject COP-BCOM distances as a proportion of subject's dominant leg length (see 3.2 above).
12. Export data for statistical analysis using the **Copy to Clipboard** functionality or by exporting files in other available native formats.

8. Lab-specific Normative Value Calculations

1. Calculate mean (± 1 SD) intra and inter-subject values for both actual COP-BCOM distances and normalized values as proportions of subjects' dominant lower limb length.
2. Calculate coefficients of variation (COV) for mean inter-subject data.
3. Calculate intra-subject variation per event using two-way mixed effects model intra-class correlation coefficients (ICC$_{3,1}$), and the measurement error[32].

Representative Results

All subjects rose with their feet placed on the twin force platforms, leading with their non-dominant limb as instructed. Normal gait was observed with subjects stepping cleanly onto the other platforms and 3D optical-based motion analysis successfully tracked whole body movement during 5 repeated goal-orientated STSW tasks rising from 120% KH. Simultaneous COP and BCOM mediolateral (ML) and anteroposterior (AP) displacements between seat-off and IC2 (100% STSW cycle) comprising: rise, pause, gait initiation (GI), step 1, and step 2 are shown respectively in **Figure 5A** and **5B** for the first subject (left leg (non-dominant) lead). In the ML plane, there was negligible COP or BCOM displacement from seat-off to GI onset. However, after GI onset COP displaces leftward away from the standing limb toward the swing limb - separating from the BCOM, which displaces rightward. Then, the COP laterally displaces rightward toward the subsequent stance limb, passing beyond the BCOM rightward before toe-off. Thereafter, during steps 1 and 2, the BCOM follows a sinusoidal displacement, with the COP displacing further laterally during single limb stance (**Figure 5A**).
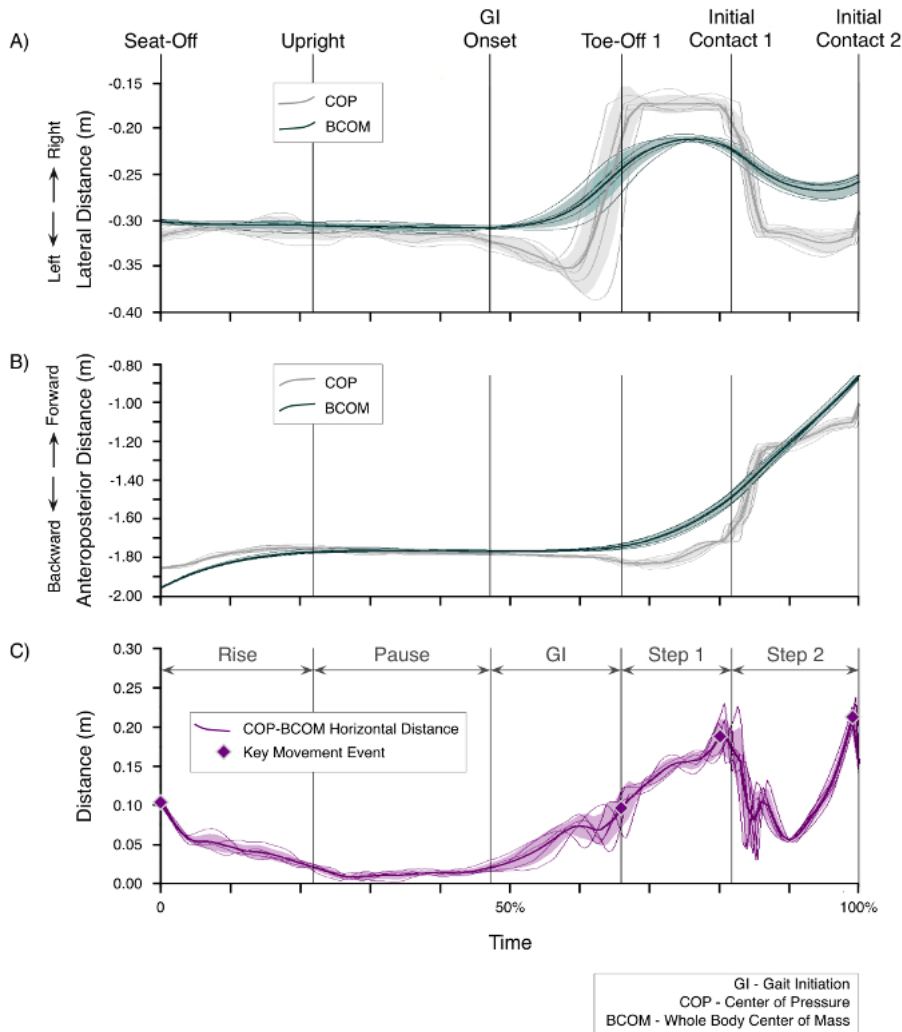
Figure 5. COP and BCOM Displacements. Panels show the first subject undertaking STSW from 120% KH with non-dominant limb-lead; in this case left-leg lead. The time axis is normalized to percentage time between seat-off and initial contact 2 (IC2). **A)** Mediolateral displacement. *Y*-axis direction labels with respect to the swing (left) leg. Lines show COP and BCOM data corresponding to each trial, the bold lines represents the mean, and shaded areas represent ±1SD around the mean. **B)** Anteroposterior displacements. *Y*-axis direction labels with respect to the swing (left) leg. Lines show COP and BCOM data corresponding to each trial, the bold lines represents the mean, and shaded areas represent ±1 SD around the mean. **C)** COP-BCOM horizontal distance. Lines show distance data corresponding to each trial, the bold line represents the mean, and shaded area represents ±1 SD around the mean. Seat-off and toe-off 1 events, and maxima during steps 1 and 2 are marked. Please click here to view a larger version of this figure.

In the AP plane, the COP at seat-off starts in front of the BCOM, and while they both move forward during rising; their separation diminishes steadily before merging at upright. After the pause phase the BCOM accelerates forwards through GI and steps 1 and 2. In contrast, the COP displaces backwards at GI onset and then forward after toe-off but remains behind the BCOM throughout step 1. The COP, however, passes in front of the BCOM during step 2 after initial contact 1 likely to correspond with the transition to single limb stance. COP forward displacement then slows and passes behind the BCOM again just before mid-stance/swing (**Figure 5B**).

The horizontal separation distance between COP and BCOM, throughout the STSW cycle, provides a composite of the planar description of COP and BCOM displacements. This approach simplifies the complex interaction of COP and BCOM displacement providing an index of positional stability (**Figure 5C**).

Intra-subject COP-BCOM separation distances were consistent at seat-off, TO1, and during step 1 and 2 by virtue of strong intraclass correlation coefficients at all 4 events. In addition, the measurement error (**Table 5**), or common standard deviation of repeated measures[32], was small: 9 mm (seat-off) and 12 mm (TO1, step 1, step 2) across all subjects. Another useful way to present measurement error is the repeatability statistic (**Table 5**). It represents the magnitude of the expected difference between 2 repeated measures 95% of the time, and is between 24 mm and 34 mm for the 4 events.

Inter-subject COP-BCOM separation distances were consistent (**Table 6**) at seat-off and TO1, in addition to during step 1 and 2. In this homogenous, healthy adult group; subject leg-length range (0.803-0.976 m (**Table 1**))[33] and variance was small (mean 0. 855 m; SD 0.051 m). Whilst it is not typical to normalize COP-BCOM distances to leg length and **Figure 6** shows negligible differences between normalized and un-normalized inter-subject mean COP-BCOM data, normalization does reduce the coefficient of variance (COV; **Table 6**).

Event	ICC (95% CI)*	S_w Distance§ (m)	Repeatability Distance† (m)
Seat-Off	0.960 (0.900-0.989)	0.009	0.024
TO1	0.977 (0.943-0.993)	0.012	0.034
Step 1	0.976 (0.940-0.993)	0.012	0.032
Step 2	0.953 (0.884-0.987)	0.012	0.034

*Intra Class Correlation Coefficient for consistency, average variation, 2 way mixed effects, (95% confidence interval)
§Measurement error, mean intra-subject SD (S_w); the square root of the mean intra-subject variance
†An estimate of the maximum difference (m) between 2 observations with 95% confidence (2.77 S_w)

Table 5: COP-BCOM Distances. Intra (5 trials) and inter-subject mean ± 1 SD data is shown as actual distances and normalized to subject non-dominant leg length for discrete distances at seat-off and TO1, and maximum distances during step 1 and step 2.

Subject	COP-BCOM Distance (m)			
	Seat-Off		TO1	
	Distance	Normalized*	Distance	Normalized
1	0.104 ±0.005	0.130 ±0.006	0.103 ±0.012	0.127 ±0.015
2	0.067 ±0.004	0.080 ±0.005	0.119 ±0.012	0.143 ±0.014
3	0.106 ±0.005	0.129 ±0.006	0.145 ±0.012	0.176 ±0.015
4	0.100 ±0.007	0.125 ±0.009	0.095 ±0.005	0.118 ±0.006
5	0.078 ±0.006	0.087 ±0.006	0.180 ±0.011	0.201 ±0.013
6	0.120 ±0.007	0.123 ±0.007	0.194 ±0.015	0.199 ±0.015
7	0.103 ±0.006	0.120 ±0.007	0.148 ±0.015	0.173 ±0.018
8	0.062 ±0.007	0.072 ±0.008	0.129 ±0.012	0.149 ±0.013
9	0.080 ±0.006	0.096 ±0.007	0.099 ±0.012	0.118 ±0.015
10	0.081 ±0.021	0.095 ±0.025	0.143 ±0.014	0.169 ±0.016
All	0.090 ±0.019	0.106 ±0.022	0.135 ±0.033	0.157 ±0.031
COV†	21.20%	20.80%	24.70%	19.70%

Subject	Maximum COP-BCOM Distance (m)			
	Step 1		Step 2	
	Distance	Normalized	Distance	Normalized
1	0.213 ±0.015	0.264 ±0.018	0.225 ±0.009	0.279 ±0.012
2	0.233 ±0.010	0.278 ±0.012	0.212 ±0.014	0.254 ±0.016
3	0.255 ±0.012	0.310 ±0.015	0.227 ±0.016	0.276 ±0.019
4	0.214 ±0.007	0.267 ±0.009	0.198 ±0.007	0.246 ±0.009
5	0.278 ±0.018	0.312 ±0.020	0.262 ±0.012	0.294 ±0.014
6	0.304 ±0.016	0.311 ±0.016	0.254 ±0.012	0.260 ±0.012
7	0.289 ±0.007	0.337 ±0.008	0.256 ±0.014	0.299 ±0.016
8	0.244 ±0.010	0.280 ±0.011	0.249 ±0.008	0.286 ±0.010
9	0.204 ±0.008	0.245 ±0.010	0.190 ±0.011	0.228 ±0.013
10	0.257 ±0.008	0.302 ±0.009	0.228 ±0.015	0.268 ±0.018
All	0.249 ±0.034	0.291 ±0.028	0.230 ±0.025	0.269 ±0.022
COV†	13.60%	9.70%	10.80%	8.30%

*Normalized COP-BCOM distance as a proportion of dominant leg length
†Coefficient of variation (SD/mean as a percentage) between subjects

Table 6: Intra-subject Variation. ICCs (95% confidence interval) and measurement error (mean intra-subject SD distance in m) and repeatability statistics[32] are shown per event.
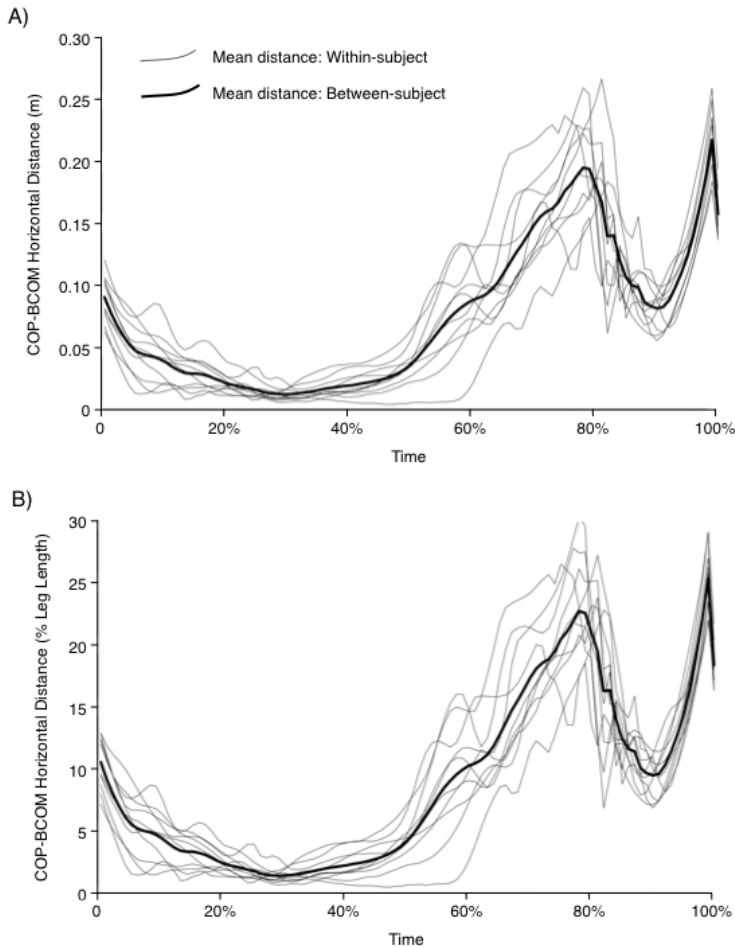
Figure 6. Within and Between-Subject COP-BCOM Distances. (A) Un-Normalized. Each line represents within-subject mean COP-BCOM distance. The bold line represents the between-subject mean distance. **(B)** Normalized to Dominant Leg Length. Each line represents within-subject mean COP-BCOM distance as a percentage of the subject's dominant leg length. The bold line represents the between-subject mean distance as a percentage of the subject's dominant leg length.

Discussion

The sit-to-stand-and-walk (STSW) protocol defined here can be used to test dynamic postural control during complex transitional movement in healthy individuals or patient groups. The protocol includes constraints that are designed to allow subjects with pathology to participate, and the inclusion of switching off the light means it is ecologically valid and goal-orientated. As it has been shown previously that lead-limb and rising from a high (120% KH) seat does not fundamentally affect task dynamics during STSW[20], the methods described here can be applied as a standard protocol. This STSW protocol has validity because compared to healthy individuals, patients find rising from low seat heights a challenge[10], tend to generate less horizontal momentum[7] and separate rising before initiating gait from a wide foot position[11] with their affected leg[7]. This paper also describes how to calculate COP and BCOM displacement during STSW, from which the horizontal separation between COP and BCOM - an index of dynamic stability[16] - can be derived between seat-off and the second step.

The results are dependent on a number of critical steps within the protocol. Firstly, the removal of artefactual light and optimal camera exposure settings is required to ensure the accuracy of optical 3D marker tracking. Secondly, attention to the capture volume when calibrating is an important consideration to further optimize motion capture accuracy. Thirdly, force plate synchronization with the motion capture system using an appropriate scale factor reduces the potential for error in the magnitude of the resultant ground reaction force vector. Fourthly, precise force plate identification in the 3D space is critical. Special care must be made when locating each plate's PRS, and validation of this accuracy must be a routine[34]. This ensures that force plate structure and rendering during post-processing is optimized for the presentation of high quality COP data. Finally, the main contributors to BCOM displacement estimation errors are inaccurate marker positioning, locating of joint centers and skin movement artifacts[35]. Thus, experience in anatomical palpation and adoption of the CAST method[18] should be considered prerequisites. Other techniques involve using fewer markers or even a singular estimator of BCOM position during gait such as sacral inertial sensors. However, this technique requires validation[36] and is of limited utility when body segment orientations deviate from those when upright *i.e.*, during rise[37]. Thus, multiple camera quantification of BCOM remains the gold standard technique for STSW.

With these steps considered in a healthy population, intra-subject variability during STSW is low, justifying averaging across trials with a high degree of confidence. Furthermore, low (healthy) inter-subject variability suggests comparison with such (lab specific) normative data would provide high sensitivity to differences induced by pathology. Whilst, inter-subject variability was low, reduced COV can be achieved by

normalizing for leg length. One aspect that warrants further investigation is the STSW pause phase. Healthy subjects self-selected a mean (± SD) pause phase of 0.84 sec (± 0.07). Whether this differs in pathological groups, and if so whether there is any effect upon stability during transition remains to be determined.

The degree of COP-BCOM separation varies during the different phases of STSW. The largest COP-BCOM distances were at seat-off, TO1, and just prior to foot contact during steps 1 and 2. These represent the biggest challenge to the postural control systems and are therefore defined as the events of interest. Decreased COP-BCOM separation is associated with increased positional stability, but indicates reduced postural stability[31]. At seat-off as the body transitions from a stable to an unstable base of support, positional stability is accomplished either by posterior positioning of the feet or anterior positioning of the trunk relative to the seat, both of which are commonly seen in functionally impaired patients[38,39]. After pause, BCOM-COP distances increase during GI; incorporating the anticipatory, postural "release" and "unloading" sub-phases[15], and a locomotor swinging limb phase. The end of GI and start of step 1 occurs at TO1; where a relative increase in COP-BCOM separation is associated with BCOM forward acceleration caused by the combined GI phases, the outcome of which is higher walking velocity[40]. Therefore, COP-BCOM distance at seat-off and TO1 represent candidate dynamic postural stability variables to be tested in pathological groups.

In addition, maximum COP-BCOM distance peaks occur consistently during steps 1 and 2 at the end of single support. These are important events to measure because steps 1 and 2 represent the period where steady-state gait is realized. Larger mean COP-BCOM distances during step 1 compared to step 2 in all but one healthy subject using the protocol were observed. Step 1 remains part of the locomotor acceleration phase before steady-state gait is reached at the end of step 2[12]. Therefore, step 1 is subject to both postural and locomotor control demands and is more positionally unstable than subsequent steps in gait; a feature supported by the increased risk of falling during every day transitional movements[41]. Step 2 is no less important as it represents the commencement of steady-state gait. Therefore, maximum COP-BCOM distances during both steps 1 and 2 phases are indicated in STSW analysis.

In conclusion, this STSW protocol extends the use of COP-BCOM horizontal separation to STSW and our preliminary results provide an initial normative data set for healthy individuals. COP-BCOM distances normalized to leg length at seat-off, TO1, and step 1 and 2 maxima during performance of a goal-orientated STSW paradigm is a novel methodology for evaluation of dynamic postural stability. It offers the possibility of deriving highly consistent normative global or local data sets that can be compared with UMN injured patients or other compromised patient groups.

Disclosures

The authors have no competing financial interests to disclose.

Acknowledgements

References

1. Duncan, P. W., Goldstein, L. B., Matchar, D., Divine, G. W., & Feussner, J. Measurement of motor recovery after stroke. Outcome assessment and sample size requirements. *Stroke.* **23** (8), 1084-1089 (1992).
2. Smith, M. T., & Baer, G. D. Achievement of simple mobility milestones after stroke. *Arch Phys Med Rehabil.* **80** (4), 442-447 (1999).
3. Langhorne, P., Bernhardt, J., & Kwakkel, G. Stroke rehabilitation. *Lancet.* **377** (9778), 1693-1702 (2011).
4. Veerbeek, J. M. *et al.* What is the evidence for physical therapy poststroke? A systematic review and meta-analysis. *PLoS One.* **9** (2), e87987 (2014).
5. Magnan, A., McFadyen, B., & St-Vincent, G. Modification of the sit-to-stand task with the addition of gait initiation. *Gait Posture.* **4** (3), 232-241 (1996).
6. Buckley, T. A., Pitsikoulis, C., & Hass, C. J. Dynamic postural stability during sit-to-walk transitions in Parkinson disease patients. *Mov Disord.* **23** (9), 1274-1280 (2008).
7. Frykberg, G. E., Aberg, A. C., Halvorsen, K., Borg, J., & Hirschfeld, H. Temporal coordination of the sit-to-walk task in subjects with stroke and in controls. *Arch Phys Med Rehabil.* **90** (6), 1009-1017 (2009).
8. Dehail, P. *et al.* Kinematic and electromyographic analysis of rising from a chair during a "Sit-to-Walk" task in elderly subjects: role of strength. *Clin Biomech (Bristol, Avon).* **22** (10), 1096-1103 (2007).
9. Buckley, T., Pitsikoulis, C., Barthelemy, E., & Hass, C. J. Age impairs sit-to-walk motor performance. *J Biomech.* **42** (14), 2318-2322 (2009).
10. Roy, G. *et al.* The effect of foot position and chair height on the asymmetry of vertical forces during sit-to-stand and stand-to-sit tasks in individuals with hemiparesis. *Clin Biomech (Bristol, Avon).* **21** (6), 585-593 (2006).
11. Kubinski, S. N., McQueen, C. A., Sittloh, K. A., & Dean, J. C. Walking with wider steps increases stance phase gluteus medius activity. *Gait Posture.* **41** (1), 130-135 (2015).
12. Jian, Y., Winter, D. A., Ishac, M. G., & Gilchrist, L. Trajectory of the body COG and COP during initiation and termination of gait. *Gait Posture.* **1** (1), 9-22 (1993).
13. Winter, D. A. Human balance and posture control during standing and walking. *Gait Posture.* **3** (4), 193-214 (1995).
14. Cavanagh, P. R. A technique for averaging center of pressure paths from a force platform. *J Biomech.* **11** (10-12), 487-491 (1978).
15. Halliday, S. E., Winter, D. A., Frank, J. S., Patla, A. E., & Prince, F. The initiation of gait in young, elderly, and Parkinson's disease subjects. *Gait Posture.* **8** (1), 8-14 (1998).
16. Hass, C. J., Waddell, D. E., Fleming, R. P., Juncos, J. L., & Gregor, R. J. Gait initiation and dynamic balance control in Parkinson's disease. *Arch Phys Med Rehabil.* **86** (11), 2172-2176 (2005).

17. Winter, D. A., Patla, A. E., Ishac, M., & Gage, W. H. Motor mechanisms of balance during quiet standing. *J Electromyogr Kinesiol.* **13** (1), 49-56 (2003).
18. Cappozzo, A., Catani, F., Croce, U. D., & Leardini, A. Position and orientation in space of bones during movement: anatomical frame definition and determination. *Clin Biomech (Bristol, Avon).* **10** (4), 171-178 (1995).
19. Dempster, W. T., Gabel, W. C., & Felts, W. J. The anthropometry of the manual work space for the seated subject. *Am J Phys Anthropol.* **17** (4), 289-317 (1959).
20. Jones, G. D., James, D. C., Thacker, M., Jones, E. J., & Green, D. A. Sit-to-Walk and Sit-to-Stand-and-Walk Task Dynamics are Maintained During Rising at an Elevated Seat-Height Independent of Lead-Limb in Healthy Individuals. *Gait Posture.* **48** 226-229 (2016).
21. *Qualysis Track Manager User Manual.* Sweden: Qualysis AB. (2011).
22. Hoffman, M., Schrader, J., Applegate, T., & Koceja, D. Unilateral postural control of the functionally dominant and nondominant extremities of healthy subjects. *J Athl Train.* **33** (4), 319-322 (1998).
23. Ren, L., Jones, R. K., & Howard, D. Whole body inverse dynamics over a complete gait cycle based only on measured kinematics. *J Biomech.* **41** (12), 2750-2759 (2008).
24. Tutorial: Building a Model. *C-Motion Wiki Documentation.* <http://www.c-motion.com/v3dwiki/index.php/Tutorial:_Building_a_Model> (2013).
25. Kainz, H., Carty, C. P., Modenese, L., Boyd, R. N., & Lloyd, D. G. Estimation of the hip joint centre in human motion analysis: a systematic review. *Clin Biomech (Bristol, Avon).* **30** (4), 319-329 (2015).
26. Harrington, M. E., Zavatsky, A. B., Lawson, S. E., Yuan, Z., & Theologis, T. N. Prediction of the hip joint centre in adults, children, and patients with cerebral palsy based on magnetic resonance imaging. *J Biomech.* **40** (3), 595-602 (2007).
27. Coda Pelvis. *C-Motion Wiki Documentation.* <http://www.c-motion.com/v3dwiki/index.php/Coda_Pelvis> (2015).
28. Bell, A. L., Brand, R. A., & Pedersen, D. R. Prediction of hip joint centre location from external landmarks. *Human movement science.* **8** (1), 3-16 (1989).
29. Eames, M. H. A., Cosgrove, A., & Baker, R. Comparing methods of estimating the total body centre of mass in three-dimensions in normal and pathological gaits. *Human movement science.* **18** (5), 637-646 (1999).
30. Force Structures. *C-Motion Wiki Documentation.* <http://www.c-motion.com/v3dwiki/index.php?title=Force_Structures> (2015).
31. Martin, M. *et al.* Gait initiation in community-dwelling adults with Parkinson disease: comparison with older and younger adults without the disease. *Phys Ther.* **82** (6), 566-577 (2002).
32. Bland, J. M., & Altman, D. G. Measurement error. *BMJ.* **313** (7059), 744 (1996).
33. Hof, A. L. Scaling gait data to body size. *Gait Posture.* **4** (3), 222-223 (1996).
34. Holden, J. P., Selbie, W. S., & Stanhope, S. J. A proposed test to support the clinical movement analysis laboratory accreditation process. *Gait Posture.* **17** (3), 205-213 (2003).
35. Baker, R. Gait analysis methods in rehabilitation. *J Neuroeng Rehabil.* **3** 4 (2006).
36. Gregory, C. M., Embry, A., Perry, L., & Bowden, M. G. Quantifying human movement across the continuum of care: From lab to clinic to community. *J Neurosci Methods.* **231** 18-21 (2014).
37. Pai, Y. C., & Rogers, M. W. Segmental contributions to total body momentum in sit-to-stand. *Medicine and Science in Sports and Exercise.* **23** (2), 225-230 (1991).
38. Hughes, M. A., Weiner, D. K., Schenkman, M. L., Long, R. M., & Studenski, S. A. Chair rise strategies in the elderly. *Clin Biomech (Bristol, Avon).* **9** (3), 187-192, (1994).
39. Medeiros, D. L., Conceição, J. S., Graciosa, M. D., Koch, D. B., Santos, M. J., Ries, L. G. The influence of seat heights and foot placement positions on postural control in children with cerebral palsy during a sit-to-stand task. *Res Dev Disabil.* **43-44**, 1-10 (2015).
40. Breniere, Y., & Do, M. C. When and how does steady state gait movement induced from upright posture begin? *J Biomech.* **19** (12), 1035-1040 (1986).
41. Weerdesteyn, V., de Niet, M., van Duijnhoven, H. J., & Geurts, A. C. Falls in individuals with stroke. *J Rehabil Res Dev.* **45** (8), 1195-1213 (2008).